

Holographic application in cosmology: Thermodynamics of the Van der Waals cosmic fluid

Mahasweta Biswas^{1*}, Sayani Maity^{2†} and Ujjal Debnath^{1‡}

¹Department of Mathematics, Indian Institute of Engineering
Science and Technology, Shibpur, Howrah-711 103, India.

²Department of Mathematics, Techno India Salt Lake, Sector-V,
Kolkata-700 091, India.

January 19, 2022

Abstract

This paper is devoted to investigate the thermodynamic stability of a generic cosmological fluid known as Van der Waals fluid in the context of flat FRW universe. It is treated as a perfect fluid that obeys the equation of state $P = \frac{\gamma\rho}{1-\beta\rho} - \alpha\rho^2$, $0 \leq \gamma < 1$, where ρ stands for energy density and P stands for pressure of the fluid. In this regard, we discuss the behavior of physical parameters to analyze the evolution of the universe. We investigate whether the cosmological scenario fulfills the third law of thermodynamics using specific heat formalism. Next we discuss the thermal equation of state and by means of adiabatic, specific heat and isothermal conditions from classical thermodynamics we examine the thermal stability.

1 Introduction

The observations like Type Ia supernova [1, 2, 3, 4], the large scale structure [5, 6, 7, 8], cosmic microwave background (CMB) [9, 10, 11] indicate that the universe endures an accelerating expansion. The source of this phenomenon is suspected to be an exotic fluid that violates strong energy condition and possesses a large negative pressure, dubbed as dark energy. According to Planck's observational data [12] about 68.3 percent of the total cosmic budget is occupied by Dark energy, while about 26.8 percent is filled with dark matter and about 4.9 percent is usual baryonic matter. There have been a prolonged attempt to reconcile the physical nature of dark energy. An overwhelming flood of dynamical dark energy models such as quintessence, tachyon [13], ghost [14], k-essence [15], fermionic field [16, 17, 18], phantom [19], Chaplygin gas [20], holographic dark energy (HDE) [21, 22, 23], new agegraphic dark energy (NADE) [24, 25] and modified gravity models such as f(R) gravity [26, 27], f(T) gravity [28, 29, 30], Hořava-Lifshitz gravity [31, 32, 33, 34] have been proposed in literature.

*mahasweta.bsc11@gmail.com

†sayani.maity88@gmail.com

‡ujjaldebnath@gmail.com

Like Chaplygin gas family, another single-component fluid known as Van der Waals fluid [35] has attracted much attention for unification of different fluid. The main feature of this model is to reproduce the accelerated and matter-dominated phases with a single component. The perfect fluid equation of state is not realistic in describing the all the phases of the evolution of the universe. The properties of Van der Waals fluid have been analyzed in [36]. It is indeed the holographic description of the dark energy, so by having information about the Van der Waals fluid we can obtain knowledge about the accelerating expansion of universe. In [37, 38] a mixture of two fluids, taking the Van der Waals fluid as dark energy and the perfect gas equation of state for the matter, have been considered to get a whole dynamics of the universe. In Ref. [39], a toy model of the Universe is considered with generalized ghost dark energy, Van der Waals fluid and some modified fluids. They have studied the unusual connection among different fluids. Although there have been a lot of work [40, 41, 42] discussing various aspects of Van der Waals fluid in the standard cosmological model with observations, there has not been done a full thermodynamic constraints of Van der Waals fluid. Thermodynamics of Chaplygin gas model has been studied by Myung [43]. Santos et al [44, 45] have studied the thermodynamic stability of the generalized and modified Chaplygin gas models. Thermodynamics of Modified Chaplygin Gas and Tachyonic Field have been analyzed in ref. [46]. Thermodynamic stability of generalized cosmic Chaplygin gas has been studied by Sharif et al [47]. Motivated by these works, here, we examine the thermodynamic stability of Van der Waals fluid in the background of a flat FRW universe.

The paper is organized as follows. In section 2, we study the behavior of pressure, EoS parameter, deceleration parameter and also analyze the stability using the sign of square speed of sound. In section 3, we study the thermodynamic stability of Van der Waals fluid. We devote the last section for summarization of the results.

2 Physical Features of Van der Waals Fluid

Here we assume the flat Friedmann-Robertson-Walker (FRW) model of the universe represented by the following line element:

$$ds^2 = -dt^2 + a^2(t)(dr^2 + r^2d\theta^2 + r^2\sin^2\theta d\phi^2), \quad (1)$$

where $a(t)$ is the scale factor. Now we assume the equation of state for Van der Waals fluid as in the form [35]

$$P = \frac{\gamma\rho}{1 - \beta\rho} - \alpha\rho^2, 0 \leq \gamma < 1, \alpha = 3p_c\rho_c^{-2}, \beta = (3\rho_c)^{-1}, \quad (2)$$

where ρ and P represent the energy density and pressure of the Van der Waals fluid. Here ρ_c and p_c represent the critical density and the critical pressure of the Van der Waals fluid at critical point. The above equation reduces to the perfect fluid case in the limit $\alpha, \beta \rightarrow 0$. The energy density of the fluid can be written in the form:

$$\rho = \frac{U}{V}, \quad (3)$$

where U is the internal energy and V is the volume. From classical thermodynamics, the relation between U , V and P can be written in the form [47, 48]

$$\frac{dU}{dV} = -P. \quad (4)$$

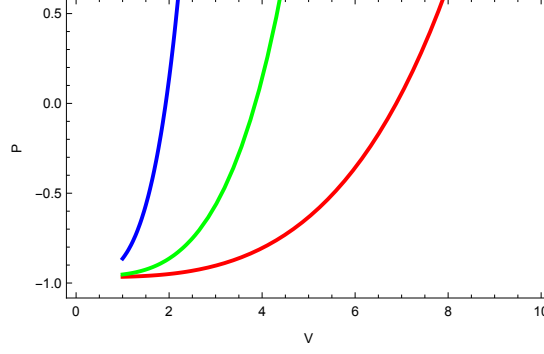


Fig.1

Figure 1: Plots of P versus V for $\gamma = 0.7, \beta = 1, \alpha = 20$ and $k = 5$ (blue curve), $k = 10$ (red curve) and $k = 20$ (green curve).

From equations (2) - (4), we get the following first order ordinary differential equation

$$\frac{dU}{dV} + \frac{\gamma U}{1 - \beta \frac{U}{V}} = \alpha \left(\frac{U}{V} \right)^2. \quad (5)$$

Assuming the binomial expansion upto first order, we obtain the approximate solution

$$U \approx V \left[\frac{(\alpha + \beta) + \sqrt{(\alpha + \beta)^2 - 4(1 + \gamma)\{\alpha\beta - (\frac{V}{k})^{2(1+\gamma)}\}}}{2\{\alpha\beta - (\frac{V}{k})^{2(1+\gamma)}\}} \right], \quad (6)$$

where k is an integration constant ($\neq 0$) which is either universal constant or a function of entropy (S). The above solution provides the solution of energy density as

$$\rho = \left[\frac{(\alpha + \beta) + \sqrt{(\alpha + \beta)^2 - 4(1 + \gamma)\{\alpha\beta - (\frac{V}{k})^{2(1+\gamma)}\}}}{2\{\alpha\beta - (\frac{V}{k})^{2(1+\gamma)}\}} \right] \quad (7)$$

For small volumes ($V \approx 0$), the energy density of the Van der Waals fluid behaves like

$$\rho = \left[\frac{(\alpha + \beta) + \sqrt{(\alpha + \beta)^2 - 4(1 + \gamma)\alpha\beta}}{2\alpha\beta} \right] \quad (8)$$

with the condition $(\alpha + \beta)^2 \geq 4(1 + \gamma)\alpha\beta$ and hence the minimum value of ρ is $\rho_{min} = \sqrt{\frac{1+\gamma}{\alpha\beta}}$. Now we will discuss different physical parameters of the model.

2.1 Pressure

From equations (2) and (7), we obtain the expression pressure in terms of V as in the following form:

$$P = \frac{\gamma[(\alpha + \beta) + \sqrt{(\alpha + \beta)^2 - 4(1 + \gamma)\{\alpha\beta - (\frac{V}{k})^{2(1+\gamma)}\}}]}{\alpha\beta - [\beta^2 + 2(\frac{V}{k})^{2(1+\gamma)} + \beta\sqrt{(\alpha + \beta)^2 - 4(1 + \gamma)\{\alpha\beta - (\frac{V}{k})^{2(1+\gamma)}\}}]} - \alpha \left[\frac{(\alpha + \beta) + \sqrt{(\alpha + \beta)^2 - 4(1 + \gamma)\{\alpha\beta - (\frac{V}{k})^{2(1+\gamma)}\}}}{2[\alpha\beta - (\frac{V}{k})^{2(1+\gamma)}]} \right]^2 \quad (9)$$

The trajectory of pressure given by the above equation against volume is drawn in figure 1 for different values of $k = 5, 10, 20$. Figure shows the positive and negative behavior of pressure. It is observed that the accelerating universe at small volume tends to decelerated phase of universe at large volume.

2.2 EoS Parameter

From equations (2) and (7), we obtain the equation of state parameter in terms of V as in the following form:

$$\begin{aligned} \omega = \frac{P}{\rho} &= \frac{2\gamma[\alpha\beta - (\frac{V}{k})^{2(1+\gamma)}]}{\alpha\beta - [\beta^2 + 2(\frac{V}{k})^{2(1+\gamma)} + \beta\sqrt{(\alpha + \beta)^2 - 4(1 + \gamma)\{\alpha\beta - (\frac{V}{k})^{2(1+\gamma)}\}}]} \\ &\quad - \alpha \left[\frac{(\alpha + \beta) + \sqrt{(\alpha + \beta)^2 - 4(1 + \gamma)\{\alpha\beta - (\frac{V}{k})^{2(1+\gamma)}\}}}{2[\alpha\beta - (\frac{V}{k})^{2(1+\gamma)}]} \right] \\ &= \begin{cases} \gamma, & V \gg k \\ -1, & V \ll k. \end{cases} \end{aligned} \quad (10)$$

The EOS parameter ω is drawn in figure 2 for different values of $k = 5, 10, 20$. The EOS parameter transits from -1 to positive values as volume increases. That means it yields cosmological constant model for small volume, then it generates the quintessence region and goes to positive region (tends to γ).

2.3 Deceleration Parameter

The deceleration parameter is given by

$$\begin{aligned} q = \frac{1}{2} + \frac{3P}{2\rho} &= \frac{1}{2} + \frac{3\gamma[\alpha\beta - (\frac{V}{k})^{2(1+\gamma)}]}{\alpha\beta - [\beta^2 + 2(\frac{V}{k})^{2(1+\gamma)} + \beta\sqrt{(\alpha + \beta)^2 - 4(1 + \gamma)\{\alpha\beta - (\frac{V}{k})^{2(1+\gamma)}\}}]} \\ &\quad - \alpha \left[\frac{(\alpha + \beta) + \sqrt{(\alpha + \beta)^2 - 4(1 + \gamma)\{\alpha\beta - (\frac{V}{k})^{2(1+\gamma)}\}}}{2[\alpha\beta - (\frac{V}{k})^{2(1+\gamma)}]} \right] \\ &= \begin{cases} \frac{1}{2} + \frac{3}{2}\gamma, & V \gg k \\ -1, & V \ll k. \end{cases} \end{aligned} \quad (11)$$

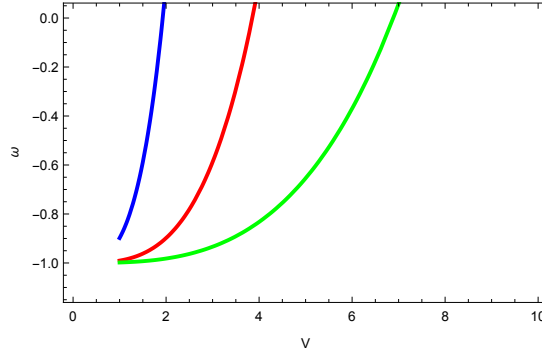


Fig.2

Figure 2: Plots of ω versus V for $\gamma = 0.7, \beta = 1, \alpha = 20$ $k = 5$ (blue curve), $k = 10$ (red curve) and $k = 20$ (green curve).

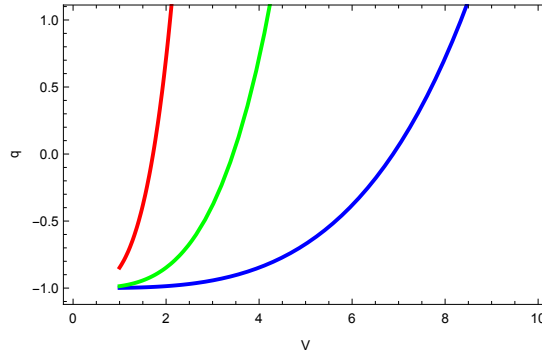


Fig.3

Figure 3: Plots of q versus V for $\gamma = 0.7, \beta = 1, \alpha = 20$ $k = 5$ (blue curve), $k = 10$ (red curve) and $k = 20$ (green curve).

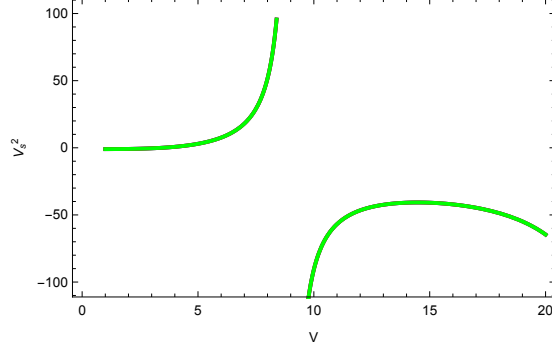


Fig.4

Figure 4: Plots of V_s^2 versus V for $\gamma = 0.7, \beta = 1, \alpha = 20$ $k = 5$ (blue curve), $k = 10$ (red curve) and $k = 20$ (green curve).

Figure 3 presents the trajectories of the deceleration parameter q against V for different values of k . From the graph we can see that q increases from -1 to the positive value (tends to $\frac{1+3\gamma}{2}$). It describes acceleration at small volumes whereas at large volume, it exhibits decelerating behavior for different values of k . So, a transition from accelerating to decelerating universe is observed. It shows $q \rightarrow -1$ with decreasing V i.e it yields cosmological constant model as $V \rightarrow 1$.

2.4 Square Speed of Sound

To discuss the classical stability of the model, we need to obtain the square speed of sound which is given by

$$\begin{aligned}
 V_s^2 = \left(\frac{\partial P}{\partial \rho} \right)_S &= \frac{4\gamma \left[\alpha\beta - \left(\frac{V}{k} \right)^{2(1+\gamma)} \right]^2}{\left[\alpha\beta - \left\{ \beta^2 + 2\left(\frac{V}{k} \right)^{2(1+\gamma)} + \beta \sqrt{(\alpha + \beta)^2 - 4(1 + \gamma) \left\{ \alpha\beta - \left(\frac{V}{k} \right)^{2(1+\gamma)} \right\}} \right\} \right]^2} \\
 &\quad - 2\alpha \frac{(\alpha + \beta) + \sqrt{(\alpha + \beta)^2 - 4(1 + \gamma) \left\{ \alpha\beta - \left(\frac{V}{k} \right)^{2(1+\gamma)} \right\}}}{2 \left[\alpha\beta - \left(\frac{V}{k} \right)^{2(1+\gamma)} \right]} \\
 &= \begin{cases} \gamma, & V \gg k \\ 4 \left[\frac{\{\alpha(1+\gamma) - \beta\} \sqrt{(\alpha - \beta)^2 - 4\alpha\beta\gamma + 3\alpha\beta\gamma - (\alpha - \beta)^2}}{\{\sqrt{(\alpha - \beta)^2 - 4\alpha\beta\gamma} - \alpha + \beta\}^2} \right], & V \ll k. \end{cases} \quad (12)
 \end{aligned}$$

In figure 4 the squared speed of sound is plotted against V for different values of k . We observe that for $0 \leq V \lesssim 9$, graph shows $V_s^2 > 0$ while for $V \gtrsim 9$, graph shows $V_s^2 < 0$. So the model is classically stable for small volume and for large volume it shows unstable behavior.

3 Thermodynamic Stability of the Van der Waals Fluid

Now we will discuss the behaviour of temperature and the thermodynamic stability of the Van der Waals Fluid. To analyze the thermodynamic stability conditions and the evolu-

tion for the Van der Waals fluid, it is necessary to determine (i) if the pressure reduces through an adiabatic expansion i.e., $(\frac{\partial P}{\partial V})_S < 0$, (ii) if the pressure reduces to an expansion at constant temperature T i.e., $(\frac{\partial P}{\partial V})_T < 0$ and (iii) if the heat capacity at constant volume i.e., $C_V > 0$.

Differentiating equation (9) w.r.t. V , we obtain

$$\begin{aligned} \left(\frac{\partial P}{\partial V}\right)_S &= \frac{(1+\gamma)(\frac{V}{k})^{2(1+\gamma)}}{VX^2\sqrt{Y}} \left[(\alpha+\beta)\sqrt{Y} + 2(1+\gamma)(\frac{V}{k})^{2(1+\gamma)} - 2\gamma\alpha\beta + \beta^2 + \alpha^2 \right] \\ &\times \left[4\gamma X^2 \left(\alpha\beta - (\beta^2 + 2(\frac{V}{k})^{2(1+\gamma)} + \beta\sqrt{Y}) \right)^{-2} - \alpha X^{-1}(\alpha + \beta + \sqrt{Y}) \right] \end{aligned} \quad (13)$$

where $X = \alpha\beta - (\frac{V}{k})^{2(1+\gamma)}$ and $Y = (\alpha + \beta)^2 - 4(1 + \gamma)X$. When the volume is very small, the above equation reduces to zero, but for the large volume, we have the following expression

$$\begin{aligned} \left(\frac{\partial P}{\partial V}\right)_S &= \frac{-4(1+\gamma)\{(\beta - \alpha(1+\gamma))\sqrt{(\alpha - \beta)^2 - 4\alpha\beta\gamma} + (\alpha - \beta)^2 - 3\alpha\beta\gamma\}}{v\alpha^2\beta^2\{-\alpha + \beta + \sqrt{(\alpha - \beta)^2 - 4\alpha\beta\gamma}\}\sqrt{(\alpha - \beta)^2 - 4\alpha\beta\gamma}} \\ &\times \left[(\alpha + \beta)\sqrt{(\alpha - \beta)^2 - 4\alpha\beta\gamma} + \alpha^2 + \beta^2 - 2\alpha\beta\gamma \right]. \end{aligned} \quad (14)$$

Figure 5(a) shows that $(\frac{\partial P}{\partial V})_S < 0$ at large volumes and at small volume, it is positive and tends to zero as $V \rightarrow 0$. So, the adiabatic condition is satisfied for all the considered values of k .

The specific heat capacity in constant volume is defined by

$$C_V = T \left(\frac{\partial S}{\partial T} \right)_V, \quad (15)$$

where the temperature can be obtained by the relation [47]

$$T = \frac{\partial U}{\partial S} = \left(\frac{\partial U}{\partial k} \right) \left(\frac{\partial k}{\partial S} \right) \quad (16)$$

Differentiating (6) with respect to k , we get

$$\frac{\partial U}{\partial k} = \frac{2(1+\gamma)(\frac{V}{k})^{2(1+\gamma)}}{kX\sqrt{Y}} [V(1+\gamma) - U\sqrt{Y}] \quad (17)$$

From equations (16) and (17), we obtain

$$T = \frac{2(1+\gamma)(\frac{V}{k})^{2(1+\gamma)}}{kX\sqrt{Y}} [V(1+\gamma) - U\sqrt{Y}] \left(\frac{\partial k}{\partial S} \right) \quad (18)$$

From equation (6), we can write (in the sense of dimensional analysis) [47]

$$[k]^{(1+\gamma)} = [U][V]^\gamma \quad (19)$$

Using the relation $[U] = [T][S]$, we obtain

$$[k] = [T]^{\frac{1}{(1+\gamma)}} [U]^{\frac{1}{(1+\gamma)}} [V]^{\frac{\gamma}{(1+\gamma)}} \quad (20)$$

From this result, we get

$$k = (\tau\nu^\gamma S)^{\frac{1}{(1+\gamma)}} \quad (21)$$

where τ and ν are constants having the dimensions of temperature and volume respectively. Differentiating (21), we obtain

$$\frac{\partial k}{\partial S} = \frac{1}{(1+\gamma)} \left(\frac{\tau\nu^\gamma}{S^\gamma} \right)^{\frac{1}{(1+\gamma)}} \quad (22)$$

Using (18) and (22) we have

$$T = \frac{2B^{\frac{1}{1+\gamma}} S^{-\frac{\gamma}{1+\gamma}} \left(\frac{V}{k}\right)^{2(1+\gamma)}}{kX\sqrt{Y}} [V(1+\gamma) - U\sqrt{Y}] \quad (23)$$

where $B = \tau\nu^\gamma$. Using (6) and (21), the equation (23) becomes

$$T = -\frac{2BV^{3+2\gamma}}{X'^2\sqrt{Y'}} [(1+\gamma)X' + ((\alpha+\beta)BS + \sqrt{Y'})\sqrt{Y'}], \quad (24)$$

where $X' = B^2 S^2 X$ and $Y' = B^2 S^2 Y$. When $T = 0$, the entropy $S = 0$ which implies that third law of thermodynamics is satisfied for our Van der Waals fluid model. Differentiating eq.(24) with respect to S , we obtain

$$\begin{aligned} \frac{\partial T}{\partial S} = & \frac{2V^{3+2\gamma}B^2}{X'^3Y'^{\frac{3}{2}}} [2BS\alpha\beta\{3X'Y'(1+\gamma) - 2X'^2(1+\gamma)^2 + 2Y'^2\} + \\ & Y'^{\frac{3}{2}}(\alpha+\beta)\{4\alpha\beta B^2 S^2 - X'\} + BSX'(\alpha+\beta)^2\{(1+\gamma)X' + 2Y'\}] \end{aligned} \quad (25)$$

Now from equation (15), we have the expression of specific heat capacity as in the following form:

$$\begin{aligned} C_V = & -[X'^2Y(1+\gamma) + X'Y'^{\frac{3}{2}}\{SB(\alpha+\beta) + \sqrt{Y'}\}] \\ & \times \left(B[2BS\alpha\beta\{3X'Y'(1+\gamma) - 2X'^2(1+\gamma)^2 + 2Y'^2\} \right. \\ & \left. + Y'^{\frac{3}{2}}(\alpha+\beta)\{4\alpha\beta B^2 S^2 - X'\} + BSX'(\alpha+\beta)^2\{(1+\gamma)X' + 2Y'\}] \right)^{-1} \end{aligned} \quad (26)$$

The specific heat C_V is plotted as the function of volume V in figure 5(b) for three different values of k . The positivity of specific heat is obtained for all considered values of k . It should be noted that when temperature T is zero, the C_V vanishes, which assures the validity of third law of thermodynamics.

4 Discussions

In this work, we have studied the thermodynamic properties of cosmological fluid described by the van der Waals equation of state in the framework of flat FRW universe. The phenomena of late time accelerated expansion of the universe is studied through different physical parameters like pressure, effective EoS, deceleration parameters and squared speed of sound. Figure 1 shows the positive and negative behavior of pressure P . We have also observed that at small volume, the universe is accelerating and it evolves to decelerated

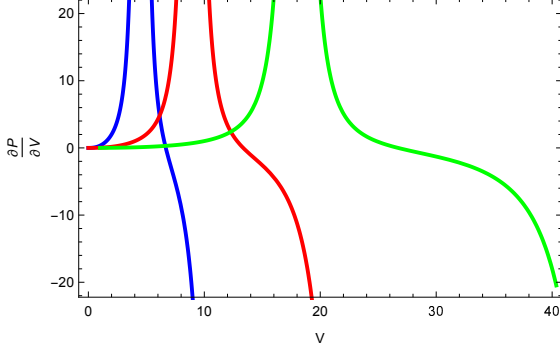


Fig.5(a)

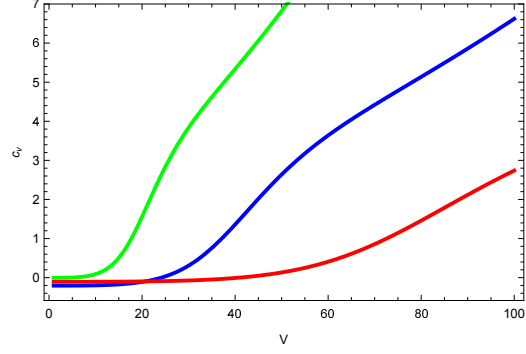


Fig.5(b)

Figure 5: Plots of $\frac{\partial P}{\partial V}$ and C_V respectively against V for $\gamma = 0.7, \beta = 1, \alpha = 20$ $k = 5$ (blue curve), $k = 10$ (red curve) and $k = 20$ (green curve).

phase at large volume. From figure 2, we have observed that the EOS parameter ω transits from -1 to positive values as volume increases. That means it yields cosmological constant model for small volume, then it generates the quintessence region and goes to positive region (tends to γ). From figure 3, we have seen that the deceleration parameter q increases from -1 to the positive value (tends to $\frac{1+3\gamma}{2}$). It describes acceleration at small volumes whereas at large volume, it exhibits decelerating behavior. So, a transition from accelerating to decelerating universe occurred. That means the deceleration parameter q yields cosmological constant model for small volume and for large volume, it crosses the quintessence region. It shows $q \rightarrow -1$ with decreasing V i.e it yields cosmological constant model as $V \rightarrow 1$. For the stability analysis of the model, the squared speed of sound V_s^2 has drawn in figure 4. We have observed that for $0 \leq V \lesssim 9$, graph shows $V_s^2 > 0$ while for $V \gtrsim 9$, graph shows $V_s^2 < 0$. So the model is classically stable for small volume and for large volume, it shows unstable behavior. Finally, we have examined the thermodynamic stability of the considered fluid using adiabatic, isothermal and specific heat conditions. From figure 5(a), we have seen that $(\frac{\partial P}{\partial V})_S < 0$ at large volumes and at small volume, it is positive and tends to zero as $V \rightarrow 0$. So, the adiabatic condition is satisfied. From figure 5(b), we have observed that the specific heat C_V is always positive. So the third law of thermodynamics is obeyed for Van der Waals fluid. For all the figures, we have assumed the considered values of k ($= 5, 10, 20$). It should be noted that when temperature T is zero, the C_V vanishes, which assures the validity of third law of thermodynamics.

References

- [1] A. G. Riess, et al., “Observational Evidence from Supernovae for an Accelerating Universe and a Cosmological Constant”, *Astron. J.* **116**, 1009 (1998).
- [2] S. Perlmutter, et al., “Measurements of Ω and Λ from 42 High-Redshift Supernovae”, *Astron. J.* **517**, 565 (1999).
- [3] P. Bernardis et al., “A Flat Universe from High-Resolution Maps of the Cosmic Microwave Background Radiation”, *Nature* **404**, 955 (2000).

- [4] R. A. Knop et al., “New Constraints on Ω_M , Ω_Λ , and w from an Independent Set of 11 High-Redshift Supernovae Observed with the Hubble Space Telescope”, *Astrophys. J.* **598**, 102 (2003).
- [5] M. Colless, et al., “The 2dF Galaxy Redshift Survey: spectra and redshifts”, *Mon. Not. R. Astron. Soc.* **328**, 1039 (2001).
- [6] M. Tegmark et al., “Cosmological parameters from SDSS and WMAP”, *Phys. Rev. D* **69**, 103501 (2004).
- [7] S. Cole et al., “The 2dF Galaxy Redshift survey : power-spectrum analysis of the final data set and cosmological implications”, *Mon. Not. R. Astron. Soc.* **362**, 505 (2005).
- [8] V. Springel, C. S. Frenk and S. M. D. White, “The large-scale structure of the Universe”, *Nature* **440**, 1137 (2006).
- [9] S. Hanany et al., “MAXIMA-1: A Measurement of the Cosmic Microwave Background Anisotropy on angular scales of 10 arcminutes to 5 degrees”, *Astrophys. J.*, **545**, L5 (2000).
- [10] C. B. Netterfield et al., “A measurement by BOOMERANG of multiple peaks in the angular power spectrum of the cosmic microwave background”, *Astrophys. J.* **571**, 604 (2002).
- [11] D. N. Spergel et al., “FIRST-YEAR WILKINSON MICROWAVE ANISOTROPY PROBE (WMAP)”, *Astrophys. J. Suppl.* **148**, 175 (2003).
- [12] U. Alam, V. Sahni and A. A. Starobinsky, “The case for dynamical dark energy revisited”, *J. Cosmol. Astropart. Phys.* **0406**, 008 (2004).
- [13] A. Sen, “Tachyon Matter”, *JHEP* **065**, 0207 (2002).
- [14] M. Malekjani, T. Naderi, and F. Pace, “Effects of ghost dark energy perturbations on the evolution of spherical overdensities”, *MNRAS* **453**, 4148 (2015).
- [15] T. Chiba, T. Okabe, and M. Yamaguchi, “Kinetically driven quintessence”, *Phys. Rev. D* **62**, 023511 (2000).
- [16] R. Myrzakulov, “Fermionic K-essence”, *arXiv: 1011.4337v4* [astro-ph.CO] (2010).
- [17] S. Maity and U. Debnath, “Correspondence between fermionic field and other dark energies”, *Astrophys. Space Sci.* **345**, 399 (2013).
- [18] S. Maity and U. Debnath, “Correspondence of F-essence with Chaplygin gas cosmology”, *Eur. Phys. J. Plus* **129**, 14 (2014).
- [19] S. Nojiri and S. D. Odintsov, “Quantum de Sitter cosmology and phantom matter”, *Phys. Lett. B* **562**, 147 (2003).
- [20] A. Yu. Kamenshchik, U. Moschella, V. Pasquier, “An alternative to quintessence”, *Phys. Lett. B* **511**, 265 (2001).
- [21] S. Weinberg, “The Cosmological Constant Problem”, *Rev. Mod. Phys.* **61**, 1 (1998).

- [22] E. J. Copeland, M. Sami and S. Tsujikawa, “Dynamics of dark energy”, *Int. J. Mod. Phys. D* **15**, 1753 (2006).
- [23] T. Padmanabhan, “Cosmological constant - the weight of the vacuum”, *Phys. Rep.* **380**, 235 (2003).
- [24] H. Wei, and R. G. Cai, “A new model of agegraphic dark energy”, *Phys. Lett. B* **660**, 113 (2008).
- [25] S. Maity, and U. Debnath, “Correspondence of F-Essence with Holographic and New Agegraphic Dark Energy Models”, *Int. J. Theor. Phys.* **55**, 698 (2016).
- [26] S. Capozziello, S. Carloni, and A. Troisi, “Quintessence without scalar fields”, *Recent Res. Dev. Astron. Astrophys.* **1**, 625 (2003).
- [27] S. M. Carroll, V. Duvvuri, M. Trodden, and M. S. Turner, *Phys. Rev. D* **70**, 043528 (2004).
- [28] R. Ferraro, and F. Fiorini, “Modified teleparallel gravity: Inflation without an inflaton”, *Phys. Rev. D* **75**, 084031 (2007).
- [29] G. R. Bengochea, and R. Ferraro, “Dark torsion as the cosmic speed-up”, *Phys. Rev. D* **79**, 124019 (2009).
- [30] E. V. Linder, “Einstein’s other gravity and the acceleration of the Universe”, *Phys. Rev. D* **81**, 127301 (2010).
- [31] P. Horava, “Quantum gravity at a Lifshitz point”, *Phys. Rev. D* **79**, 084008 (2009).
- [32] P. Horava, “Membranes at Quantum Criticality”, *JHEP* **0903**, 020 (2009).
- [33] P. Horava, “Spectral Dimension of the Universe in Quantum Gravity at a Lifshitz Point”, *Phys. Rev. Lett.* **102**, 161301 (2009).
- [34] S. Maity, and P. Rudra, “Gravitational Baryogenesis in Horava-Lifshitz gravity”, *Mod. Phys. Lett. A* **34**, 1950203 (2019).
- [35] S. Capozziello, V. F. Cardone, S. Carloni, S. De Martino, M. Falanga, A. Troisi, and M. Bruni, “Constraining Van der Waals quintessence by observations”, *JCAP* **0504**, 005 (2005).
- [36] R. C. S. Jantsch, M. H. B. Christmann, and G. M. Kremer, “The van der Waals fluid and its role in cosmology”, *IJMPD* **25**, 1650031 (2016).
- [37] G. M. Kremer, “Cosmological models described by a mixture of van der Waals fluid and dark energy”, *Phys. Rev. D* **68**, 123507 (2003).
- [38] G. M. Kremer, “Brane cosmology with a van der Waals equation of state”, *Gen. Rel. Grav.* **36**, 1423 (2004).
- [39] M. Khurshudyana and B. Pourhassan, “A Universe with a Generalized Ghost Dark Energy and Van der Waals Fluid Interacting with a Fluid”, *Int. J. Theor. Phys.* **54**, 3251 (2015).
- [40] V. F. Cardone, C. Tortora, A. Troisi, and S. Capozziello, “Beyond the perfect fluid hypothesis for the dark energy equation of state”, *Phys. Rev. D* **73**, 043508 (2006).

- [41] B. Saha, “Anisotropic Cosmological Models with Perfect Fluid and Dark Energy Reexamined”, *Int. J. The. Phy.* **45**, 952 (2006).
- [42] M. Khurshudyana, B. Pourhassan, and E. O. Kahya, “Interacting two-component fluid models with varying EoS parameter”, *Int. J. Geom. Met. Mod. Phys.* **11**, 1450061 (2014).
- [43] Y. S. Myung, “Thermodynamics of Chaplygin gas”, *Astrophys. Space Sci.* **335**, 561 (2011).
- [44] F. C. Santos, M. L. Bedranb, V. Soares, “On the thermodynamic stability of the generalized Chaplygin gas”, *Phys. Lett. B* **636**, 86 (2006).
- [45] F. C. Santos, M. L. Bedranb, V. Soares, “On the thermodynamic stability of the modified Chaplygin gas”, *Phys. Lett. B* **646**, 215 (2007).
- [46] S. Bhattacharya and U. Debnath, “Thermodynamics of Modified Chaplygin Gas and Tachyonic Field”, *Int. J. Theor. Phys.* **51**, 565 (2012).
- [47] M. Sharif and S. Ashraf, “Thermodynamics of Modified Cosmic Chaplygin Gas”, *Ad. High Energy Phys.* 2018, 8949252 (2018).
- [48] L. D. Landau, and E. M. Lifschitz, “Course of Theoretical Physics”, *Statistical Physics, third ed.*, **5**, (1984).